Scientific paper

Low-temperature Heat Capacities and Thermochemistry on the Complex of Erbium Perchlorate with L-α-Glycine $[Er_2(L\text{-}Gly)_2(H_2O)_{12}](ClO_4)_6 \cdot 4H_2O(s)$

You-Ying Di[a,*] and Zhi-Cheng Tan[b]

[a] *College of Chemistry and Chemical Engineering, Liaocheng University, Liaocheng 252059, Shandong Province, P. R. Cnina*

[b] *Thermochemistry Laboratory, Dalian Institute of Chemical Physics, Chinese Academy of Sciences, Dalian 116023, P. R. China*

** Corresponding author: Tel: +86-635-8538299, Fax: +86-635-8239121*
E-mail: yydi@lcu.edu.cn, diyouying@126.com

Received: 03-11-2006

Abstract

A coordination compound of erbium perchlorate with L-α-glycine, $[Er_2(Gly)_2(H_2O)_{12}]\ (ClO_4)_6 \cdot 4H_2O(s)$, was synthesized. By chemical analysis, elemental analysis, FTIR, TG/DTG, and comparison with relevant literature, its chemical composition and structure were established. The purity was found to be >99.0%, without melting point. Low-temperature heat capacities were measured by a precision automated adiabatic calorimeter over the temperature range from 78 to 372 K. An obvious endothermic peak in the heat capacity curve was observed over the temperature region of 275–296 K, which was ascribed to a solid-to-solid phase transition according to the results of TG/DTG analysis. The temperature T_{tr}, the enthalpy $\Delta_{tr}H_m$ and the entropy $\Delta_{tr}S_m$ of the phase transition for the compound were determined to be, T_{trs} = (283.315 ± 0.061) K, (11.026 ± 0.059) kJ mol^{-1} and (38.918 ± 0.206) J K^{-1} mol^{-1}. Two polynomial equations of heat capacities as a function of the temperature in the regions of 78–275 K and 296–372 K were fitted by the least square method, respectively. The mechanism about thermal decomposition of the complex was deduced on the basis of the TG/DTG analysis. In accordance with Hess law, the standard molar enthalpy of formation for the complex was determined as $\Delta_f H_m^o$= –(7794.40±1.01) kJ mol^{-1}, by an isoperibol solution-reaction calorimeter.

Keywords: Complex of erbium perchlorate with L-α-glycine; Adiabatic calorimetry; Low-temperature heat capacity; Isoperibol solution-reaction calorimetry; Standard molar enthalpy of formation

1. Introduction

The complexes of the rare earth elements with L-α-amino acids have the efficacies of sterilization, disinfection, resisting blood coagulation, reducing blood and sugar, and so on, which make them have wide application prospective in medicine, agriculture, biology and other fields.[1–3] These applications are related to the interaction of the rare earth ions with protein, amino acids or other biological active substances. In recent decades, the study on the complexes of the rare earths with amino acids has been one of the research foci in biological inorganic chemistry. Many reports existent in the literatures are mainly involved in the synthesis and determination of the crystal structures of these complexes.[4] Until now, few of reports about low-temperature heat capacities and thermochemical study for them were found. It is well-known that heat capacity of the substances is a basic data indispensable to theoretical research and application development pertinent to them.

In the present work, we referred to correlative literature, prepared a complex of erbium perchlorate with L-α-glycine, $[Er_2(Gly)_2(H_2O)_{12}](ClO_4)_6 \cdot 4H_2O(s)$, characterized its structure and composition, measured low-temperature heat capacity in the temperature region of 78–372 K, calculated thermodynamic parameters about the solid-solid phase transition. The mechanism of thermal decomposition of the complex has been studied by TG/ΔTG tech-

nique. In addition, standard molar enthalpy of formation of the complex has been determined by an isoperibol solution-reaction calorimeter.

2. Experimental

2. 1. Synthesis and Characterization of the Sample $[Er_2(L\text{-}Gly)_2(H_2O)_{12}](ClO_4)_6 \cdot 4H_2O(s)$

The sample was synthesized by the method given in the literature.[5] A solution containing 20 mmol of $Er(ClO_4)_3$ from the aqueous solution of $Er(ClO_4)_3$ with the concentration of 0.988 mol L^{-1} was taken. The solution was added up to 100 ml by use of the distilled water, 20 mmol of L-glycine was added to the solution, it was dissolved by adequate stirring, and pH value of the solution was adjusted to 4.0. The temperature was kept constant at 50 °C in water bath. The solution was stirred for 3 h and concentrated in water bath up to change into a saturated solution, slow and natural evaporation was conducted at room temperature, and 40 days later, pink crystal was separated out. Crystal was taken out from the solution, put it into an ether-water mixed solution to bath for three times, vacuum drying was done for 4 h, and about 6.0 g of the laurel-green sample was obtained. The final sample was placed into a desiccator containing P_4O_{10} as the desiccant and ready for use.

The content of element Er was determined with five parallel tests by EDTA chemical titration. The contents of the elements C, N and H were measured by use of elemental analysis device (model, 1160; made in Italy). These values of calculated and measured results have been listed in Table 1. It can be obviously seen from Table 1 that experimental values were consistent with those obtained from theoretical calculation. The purity of the sample can be calculated from the ratio of the real content to the theoretical content of the element Er, 27.25 / 27.36 = 99.60%. The composition and structure of the compound were further verified by TG/DTG technique. The melting point was measured by a micro melting point device, no melting was found, and the sample can stably exist in the temperature range of 20–40 °C. The sample can be easily dissolved in the water, but can not be dissolved in acetone or ether. Additionally, FTIR was done in order to check up the coordination modes of Er with L-glycine or the water in the complex, as shown in Figure 1. Data of IR characteristic absorptions of main groups of L-α-glycine and target complex (cm^{-1}) have been listed in Table 2. It can be found out that characteristic vibration absorptions of –COOH $–NH_3^+$ and $–COO^-$ of L-α-glycine clearly appeared in Figure 1. This indicated that free ligand existed in the form of $NH_3^+(CH_2COO^-$. FTIR of the complex retained the weak absorption of NH_3^+, but absorption of –COOH disappeared basically, and characteristic vibration absorption of $–COO^-$ appeared. $\nu^{as}_{(COO^-)}$ and $\nu^{s}_{(COO^-)}$ were shifted to low wave numbers. The stretching ($\nu^{s}_{NH_3^+}$ and $\nu^{as}_{NH_3^+}$) and bending ($\delta^{s}_{NH_3^+}$ and $\delta^{as}_{NH_3^+}$) vibration absorptions of $–NH_3^+$ were also shifted to low wave number from free ligand to the complex. It can be seen from big shift that $–NH_3^+$ was also in for the coordination. These results indicated that the amino acids as the ligand in the complex were coordinated with the rare earth Er^{3+} by means of $–COO^-$ and $–NH_3^+$. In addition, it can be found out from FTIR that free ligand had not the absorption $\nu_{O–H}$ of the water molecule, but the complex had the very strong absorption of the water ($\nu_{O–H}$), and took a very wide and scattered absorption peak of $\nu_{O–H}$, which indicated that both the crystal and coordinated waters existed in the complex.

Table 1. The results of chemical and elementary analysis for Er, C, N and H of the sample

Elements	Er / %	C / %	H / %	N / %
Measured	24.35	3.49	3.07	2.03
Calculated	24.42	3.51	3.09	2.05

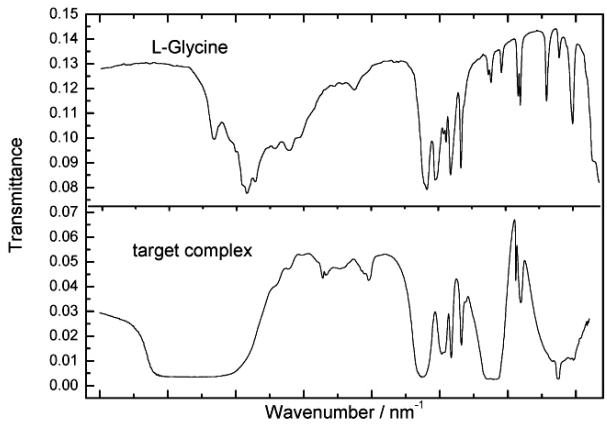

Figure 1. FTIR of L-α-glycine and target complex (cm^{-1})

TG-ΔTG technique was applied to determine the stability of the compound. It can be seen from the TG-ΔTG curves shown in Figure 2 that three obvious mass-loss processes took place with the increase of the temperature. First mass-loss took place in the temperature range of 40–155 °C (the maximum differential mass-loss temperature in DTG was at 115.1 °C) and the mass-loss percentage was 10.70%, which was in agreement with the theoretical percent content (10.51%) of three crystal water molecules in the compound. Second mass-loss process happened over the temperature region of 159–210 °C (the maximum differential mass-loss temperature in DTG was at 205.3 °C) and the mass-loss percentage was 9.37%, which agreed with the theoretical mass-loss (9.20%).

Table 2. Data of IR absorption of main groups of L-α-glycine and target complex (cm^{-1}) [a]

Compound	ν_{O-H} (H_2O)	$\nu^{as}_{NH_3^+}$	$\nu^{s}_{NH_3^+}$	$\nu^{s}_{(COO)^-}$	$\delta^{as}_{NH_3^+}$	$\delta^{as}_{NH_3^+}$	$\nu^{as}_{(COO)^-}$ (–COOH)	ν_{O-H}
L-α-Gly	/	3180 (m, s)	2910 (vs)	1670 (vs)	1510 (vs)	1450 (s)	1410 (s)	2650 (m)
Complex	3000–3500 0 (br, vs)	2710 (m)	2680 (m)	1640 (vs)	1470 (vs)	1380 (vs)	1350 (s)	/

[a] br – broad peak; s – strong; m – middle; w – very weak; vs – very strong; ν – stretching vibration; δ – bending vibration; s – symmetrical; as – asymmetrical

Third mass-loss process took place in the temperature region of 215–320 °C (the maximum differential mass-loss temperature in DTG was at 294.9 °C) and the mass-loss percentage was 12.39%, which agreed with the theoretical mass-loss (12.28%). Fourth mass-loss process took place in the temperature region of 323–450 °C (the maximum differential mass-loss temperature in DTG was at 428.5 °C) and the mass-loss percentage was 28.25%, which agreed with the theoretical mass-loss (28.04%).

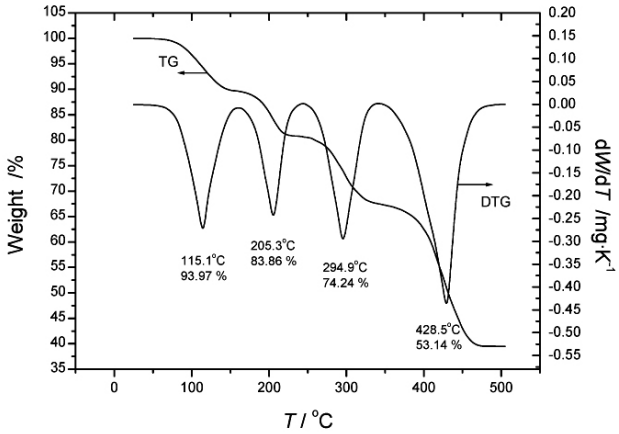

Figure 2. TG/ΔTG curve of the complex $[Er_2(L\text{-}Gly)_2(H_2O)_{12}](ClO_4)_6 \cdot 4H_2O(s)$

The mechanism of thermal decomposition of the compound was derived from the results of TG-DTG analysis as follows,

$$[Er_2(L\text{-}Gly)_2(H_2O)_{12}](ClO_4)_6 \cdot 4H_2O \xrightarrow[10.70\%\ (10.51\%)]{40\text{ - }115.1\text{ - }155\ ^oC} [Er_2(Gly)_2(H_2O)_8](ClO_4)_6$$

$$\xrightarrow[9.37\%\ (9.20\%)]{159\text{ - }205.3\text{ - }210\ ^oC} [Er_2(Gly)_2(H_2O)](ClO_4)_6 \xrightarrow[12.39\%\ (12.28\%)]{215\text{ - }294.9\text{ - }320\ ^oC} [Er_2(H_2O)](ClO_4)_4$$

$$\xrightarrow[28.25\%\ (28.04\%)]{323\text{ - }428.5\text{ - }450\ ^oC} ErOCl \cdot ErCl_3$$

in which the values of the temperatures above the arrows were corresponding to the starting, the maximum differential mass-loss and the ending decomposition temperatures of the every mass-loss process, respectively, the values below the arrows were the mass-loss percentages of the every decomposition process, the values in the brackets were obtained from theoretical calculation based on the chemical formula of the compound.

2. 2. Adiabatic Calorimetry

A high-precision automatic adiabatic calorimeter was used to measure the heat capacities over the temperature range 78 ≤ (*T*/K) ≤ 372. The calorimeter was established in the Thermochemistry laboratory of Dalian Institute of Chemical Physics, Chinese Academy of Sciences in P.R. China. The principle and structure of the adiabatic calorimeter were described in detail elsewhere.[6] Briefly, the calorimeter mainly comprised a sample cell, a platinum resistance thermometer, an electric heater, inner and outer adiabatic shields, two sets of six-junctions chromel-constantan thermopiles installed between the calorimetric cell and the inner shield and between the inner and outer shields, respectively, and a high vacuum can. The miniature platinum resistance thermometer (IPRT No.2, produced by Shanghai Institute of Industrial Automatic Meters, 16 mm in length, 1.6 mm in diameter and a nominal resistance of 100 Ω) was applied to measure the temperature of the sample. The thermometer was calibrated on the basis of ITS-90 by the Station of Low-Temperature Metrology and Measurements, Academia Sinica. The electrical energy introduced into the sample cell and the equilibrium temperature of the cell after the energy input were automatically recorded by use of the Data Acquisition / Switch Unit (Model 34970A, Agilent, USA), and processed on line by a computer.

To verify the accuracy of the calorimeter, the heat-capacity measurements of the reference standard material, α-Al_2O_3, were made over the temperature range 78 ≤ (*T*/K) ≤ 373. The sample mass used was 1.6382 g, which

was equivalent to 0.0161 mol based on its molar mass, $M(Al_2O_3)$ = 101.9613 g mol^{-1}. Deviations of the experimental results from those of the smoothed curve lied within ± 0.2%, while the uncertainty was within ± 0.3%, as compared with the values given by the former National Bureau of Standards over the whole temperature range.[7]

Heat-capacity measurements were continuously and automatically carried out by means of the standard method of intermittently heating the sample and alternately measuring the temperature. The heating rate and temperature increments were generally controlled at (0.1 to 0.4) K min^{-1} and (1 to 3) K. The heating duration was 10 min, and the temperature drift rates of the sample cell measured in an equilibrium period were always kept within (10^{-3} to 10^{-4}) K min^{-1} during the acquisition of all heat-capacity data. The data of heat capacities and corresponding equilibrium temperature have been corrected for heat exchange of the sample cell with its surroundings. The sample mass used for calorimetric measurements was 2.9018 g, which was equivalent to 2.236 · 10^{-3} mol in terms of its molar mass, M = 1369.68 g mol^{-1}.

2. 3. Isoperibol Solution-reaction Calorimetry

The isoperibol solution-reaction calorimeter consisted primarily of a precision temperature controlling system, an electric energy calibration system, the calorimetric body, the electric stirring system, the thermostatic bath made by transparent silicate glass, the precision temperature measuring system and the data acquisition system. The principle and structure of the calorimeter were described in detail elsewhere.[8, 9]

The reliability of the calorimeter was verified previously by measuring the dissolution enthalpies of THAM (NBS 742a, USA) in 0.1 mol dm^{-3} hydrochloric acid and KCl (calorimetrically primary standard) in double distilled water at T = 298.15 K. Relative deviations of the measurement results from the literature values were within 0.3%.[10]

In all dissolution experiments, 1 mol dm^{-3} HCl was chosen as the beginning calorimetric solvent for measuring the dissolution enthalpies of the {2$ErCl_3 \cdot 6H_2O$(s) + 2Gly(s) + 6$NaClO_4 \cdot H_2O$(s)} and the {[$Er_2(Gly)_2(H_2O)_{12}$]$(ClO_4)_6 \cdot 4H_2O$(s) + 6NaCl(s)}, respectively.

The solid $ErCl_3 \cdot 6H_2O$(s), Gly(s) and $NaClO_4 \cdot H_2O$(s) were ground within an agate mortar into fine powder, respectively. A mixture of about 0.382 g of $ErCl_3 \cdot 6H_2O$(s), about 0.075 g of Gly(s) and about 0.421 g of $NaClO_4 \cdot H_2O$(s) at mole ratio of $n(ErCl_3 \cdot 6H_2O)$: n(Gly) : $n(NaClO_4 \cdot H_2O)$ = 1 : 1 : 3 was dissolved in 100 ml of 1 mol dm^{-3} HCl at T = 298.15 K. The final solution obtained was designated as solution A.

The solid complex $Er_2(Gly)_2(H_2O)_{12}](ClO_4)_6 \cdot 4H_2O$(s) was dried in a vacuum desiccator in order to take off some additional adsorbing water. Then, it and NaCl(s) were respectively ground into fine powder. The dissolution enthalpy of a mixture of about 0.685 g of $Er_2(Gly)_2(H_2O)_{12}](ClO_4)_6 \cdot 4H_2O$(s) and about 0.175 g of NaCl(s) at mole ratio of n (target complex) : n (NaCl) = 1 : 6 in 100 ml of 1 mol dm^{-3} hydrochloric acid was determined under the same condition as the above. The final solution obtained was named as solution A'.

Finally, UV/Vis Spectroscopy and the data of the refractive indexes were used to confirm whether solution A was in the same thermodynamic state as that of solution A'. These results have indicated that chemical components and physical-chemistry properties of Solution A were consistent with those of solution A'.

3. Results and Discussion

3. 1. Heat Capacity

All experimental results were listed in Table 3 and plotted in Figure 3. It can be seen from Figure 3 that an obvious endothermic peak appeared in the temperature region from 275 to 296 K. No melting took place in the temperature range, as shown in the measurement by micro melting point device. No mass-loss phenomenon came forth in the temperature region by TG/DTG analysis. Therefore, the endothermic peak may be attributed to a solid-solid phase transition of the sample.

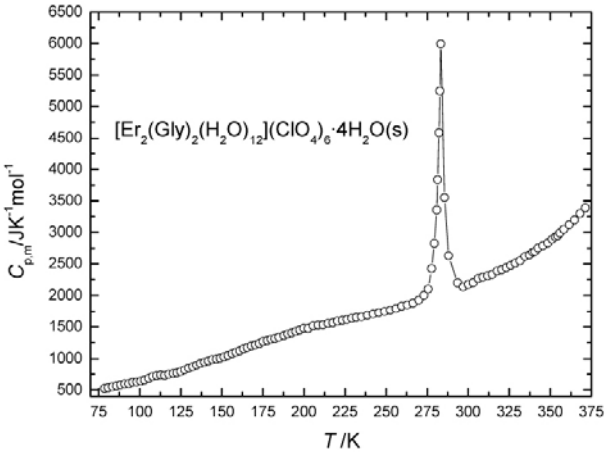

Figure 3. Experimental molar heat capacity curve of the complex $[Er_2(L\text{-}Gly)_2(H_2O)_{12}](ClO_4)_6 \cdot 4H_2O$(s) with the temperature (K)

The heat capacity of the sample increased with the temperature in the temperature regions of 78–275 K and 296–372 K. The heat capacity increased with the faster speed after T = 315 K, which may be related to the slow dehydration of the coordination compound, the water vapor cannot be given out and the dehydration process was partly restrained due to the sealing of the sample cell during the experiment. Effect of the vapor pressure on the experimental heat capacities has been considered, was within the range of the calorimetric precision and may be

Table 3. Experimental molar heat capacities of $[Er_2(L\text{-}Gly)_2(H_2O)_{12}](ClO_4)_6\ 4H_2O(s)$ (M = 1369.68 g mol^{-1})

T	$C_{p\,m}$	T	$C_{p\,m}$	T	$C_{p\,m}$
K	J K^{-1} mol^{-1}	K	J K^{-1} mol^{-1}	K	J K^{-1} mol^{-1}
78.472	521.697	170.306	1218.35	279.369	2827.16
80.864	534.098	172.739	1236.69	280.890	3355.11
83.340	550.459	175.100	1269.72	281.452	3838.53
85.848	563.302	177.608	1284.40	282.205	4587.52
88.356	579.220	179.968	1304.36	282.781	5244.28
90.790	594.495	182.329	1317.43	283.301	5993.27
93.224	596.330	184.763	1337.61	285.616	3552.29
95.659	622.018	187.861	1362.75	288.089	2628.94
98.166	623.853	190.074	1385.32	293.589	2201.69
100.601	635.872	192.508	1403.67	296.913	2137.46
102.887	653.211	194.942	1427.25	300.007	2176.55
105.469	680.734	197.449	1451.65	302.987	2204.48
107.903	711.927	199.884	1478.89	305.967	2268.70
110.337	722.936	202.613	1475.18	308.946	2291.04
112.698	733.944	205.563	1517.43	311.811	2310.59
115.205	728.440	208.588	1528.44	314.677	2335.72
117.713	748.624	211.612	1535.78	317.656	2388.78
120.295	757.798	214.563	1555.96	320.521	2408.33
122.655	768.807	217.513	1565.83	323.157	2439.05
124.942	792.661	220.464	1590.23	325.908	2475.35
127.376	818.349	223.340	1604.17	328.543	2511.65
129.737	847.706	226.217	1618.12	331.523	2550.75
132.171	868.578	229.094	1636.69	334.617	2620.56
134.679	892.982	231.897	1651.37	337.253	2640.11
136.965	922.936	235.068	1662.39	339.316	2687.58
139.399	943.119	238.609	1686.24	340.691	2695.96
141.759	961.468	242.076	1708.26	342.525	2754.59
144.120	983.486	245.616	1728.44	345.505	2793.69
146.628	992.661	249.083	1747.11	348.484	2835.58
148.988	1005.41	252.550	1768.81	351.120	2894.22
151.349	1026.33	255.908	1790.24	353.068	2930.52
153.746	1046.81	259.492	1829.33	354.445	2947.27
156.154	1075.01	262.902	1850.54	355.819	2994.75
158.537	1099.51	266.402	1880.85	358.225	3050.60
160.899	1124.10	269.890	1927.77	361.434	3123.20
163.132	1153.69	272.932	1979.76	364.758	3198.61
165.537	1174.07	275.575	2076.27	368.081	3299.13
167.942	1199.05	277.658	2497.98	371.405	3388.49

omitted. Experimental molar heat capacities in the two temperature regions were fitted to two polynomials of heat capacities with the reduced temperatures by least square fitting. (1) before the solid-solid phase transition, that is, in the region of 78–275 K,

$$C_{p,\mathrm{m}} = 1272.5386 + 889.2612x - 264.0746x^2 - \\ - 468.0971x^3 + 251.8026x^4 + 332.1040x^5 + \\ + 11.3069x^6$$

in which x was the reduced temperature, and x = (T – 176.5)/98.5. The relative deviations of the smoothed heat capacities obtained by the above equation from experimental heat capacities were within ± 0.30% except for several points around lower and upper temperature limits. (2) after the solid-solid phase transition, that is, in the region of 296–37 K,

$$C_{p,\mathrm{m}} = 2595.5808 + 564.7943x + 185.2638x^2 + \\ + 71.7182x^3 - 13.7853x^4$$

in which x was the reduced temperature, and $x = (T - 334) / 38$. The relative deviations of the smoothed heat capacities obtained by the above equation from experimental heat capacities were within ± 0.25%.

3. 2. Peak Temperature, Enthalpy and Entropy of the Solid-solid Phase Transition

The endothermic peak in the temperature range from T = 275 K to T = 296 K in the heat capacity curve was conferred to be a solid-solid phase transition from the solid I to the solid II because the substance was dehydrated in the temperature range of 40–155 °C and without a melting point. Three series of heat-capacity experiments in the temperature region of T = 250–350 K were made to confirm the reversibility and repeatability of the transition from the solid I to solid II. Before each series of measurements, the sample was cooled from T = 350 K to T = 250 K by liquid nitrogen as the coolant and introducing the helium gas to the vacuum can of the calorimeter.

The area of the peak of the solid-solid transition equaled to heat quantity absorbed by the phase transition of the sample. The molar enthalpy of the transition can be calculated from the following equation, [11]

$$\Delta_{\mathrm{tran}}H_{\mathrm{m}} = \left[Q - n\int_{T_{\mathrm{i}}}^{T_{\mathrm{trans}}} C_{P(\mathrm{s,I})}\,\mathrm{d}T - n\int_{T_{\mathrm{trans}}}^{T_{\mathrm{f}}} C_{P(\mathrm{s,II})}\,\mathrm{d}T - \int_{T_{\mathrm{i}}}^{T_{\mathrm{f}}} \overline{H}_0\,\mathrm{d}T \right] / n \qquad (1)$$

where T_{trans} – the peak temperature of the phase transition of the sample; T_{i} – the equilibrium temperature slightly below the beginning transition temperature; T_{f} – a temperature a little higher than the ending transition temperature; Q – the total energy introduced to the sample and cell when heating up from T_{i} to T_{f}; $\overline{H}_0$ – the average heat capacity of empty cell between T_i and T_f; C_p(s, I) – the heat capacity at T_i; C_p*(s, II)* is the heat capacity at T_f; n – the molar number of the sample.

The molar entropy of the phase transition can be calculated based on molar enthalpy and peak temperature of the transition by the formula,

$$\Delta_{\mathrm{trans}}S_{\mathrm{m}} = \Delta_{\mathrm{trans}}H_{\mathrm{m}} / T_{\mathrm{trans}} \qquad (2).$$

The results of T_{trans}, $\Delta_{\mathrm{trans}}H_{\mathrm{m}}$ and $\Delta_{\mathrm{trans}}S_{\mathrm{m}}$ obtained from three series of repeated heat-capacity measurements were shown in Table 4.

3. 3. The Standard Molar Enthalpy of Formation of the Complex

The complex $[Er_2(L\text{-}Gly)_2(H_2O)_{12}](ClO_4)_6 \cdot 4H_2O(s)$ was one of the products in the following reaction,

$$2ErCl_3 \cdot 6H_2O(s) + 2Gly(s) + 6NaClO_4 \cdot H_2O(s) = [Er_2(L\text{-}Gly)_2(H_2O)_{12}](ClO_4)_6 \cdot 4H_2O(s) + 6NaCl(s) + 2H_2O(l) \qquad (3).$$

The enthalpy change of the above supposed reaction and standard molar enthalpy of formation of the complex $[Er_2(L\text{-}Gly)_2(H_2O)_{12}](ClO_4)_6 \cdot 4H_2O(s)$ can be determined through a designed Hess thermochemical cycle using the experimental data of isoperibol calorimetry and other auxiliary thermodynamic data.

0.5 mmol of the complex $[Er_2(L\text{-}Gly)_2(H_2O)_{12}](ClO_4)_6 \cdot 4H_2O(s)$ was regarded as the norm, and certain amounts of reactants and other products of the reaction (3) were weighted according to their stoichiometric numbers in the supposed reaction. 100 ml of 1 mol dm^{-3} HCl (aq) was chosen as the calorimetric solvent.

If 's' = calorimetric solvent, 1 mol dm^{-3} HCl (aq), the dissolution process of the mixture of reactants in the reaction (3) was expressed into $\{2ErCl_3 \cdot 6H_2O(s) + 2Gly(s) + 6NaClO_4 \cdot H_2O(s)\}$ + 's' = solution A.

The experimental results of the process were listed in Table 5.

The dissolution process of a mixture of the products, $\{[Er_2(L\text{-}Gly)_2(H_2O)_{12}](ClO_4)_6 \cdot 4H_2O(s) + 6NaCl(s)\}$, in the reaction (3) may be expressed as follows, $\{[Er_2(L\text{-}Gly)_2(H_2O)_{12}](ClO_4)_6 \cdot 4H_2O(s) + 6NaCl(s)\}$ + 's' = solution A'.

The results of the dissolution experiments were shown in table 6.

The dilution enthalpy of $\{2H_2O(l)\}$ ($\Delta_{\mathrm{sol}}H_3$) as one of the products in the reaction (3) in the solution A' was within the range of experimental error, cannot be detected and may be omitted because the amount of $H_2O(l)$ was very small according to the stoichiometric number of $H_2O(l)$ in the reaction (3), namely, $\Delta_{\mathrm{sol}}H_3$/kJ mol^{-1} = 0.

The enthalpy change of the reaction (3), $\Delta_{\mathrm{r}}H_{\mathrm{m}}$, can be calculated in accordance with the above designed Hess thermochemical cycle and experimental results listed in Tables 5 and 6 by the following equation as follows,

Table 4. The results of the solid-solid phase transition of the compound obtained from three series of heat capacity measurements

Thermodymanic Propertites	*x*1	*x*2	*x*3	$(x\pm\sigma_a)^*$
T_{tran}/K	283.416	283.204	283.325	(283.315±0.061)
$\Delta_{\mathrm{tr}}H_{\mathrm{m}}$/kJ mol^{-1}	11.105	11.061	10.911	(11.026±0.059)
$\Delta\mathrm{tr}S_{\mathrm{m}}$/J K–1 mol^{-1}	39.183	39.057	38.511	(38.918±0.201)

* $\sigma_a = \sqrt{\sum_{i=1}^{3}(x_i - \bar{x})^2 / n(n-1)}$, in which n is the experimental number; x_i, a single value in a set of heat capacity measurements; $\bar{x}$, the mean value of a set of measurement results.

Table 5 Dissolution Enthalpy of the mixture [$ErCl_3$ $6H_2O$(s), L-Gly(s) and $NaClO_4$ H_2O(s)] at T = 298.15 K[a]

No	$W_{ErCl_3\ 6H_2O}$ (g)	W_{Gly} (g)	$W_{ErCl_3\ 6H_2O}$ (g)	ΔE_s (mV)	ΔE_e (mV)	t (s)	$\Delta_d H_1$ (kJ mol^{-1})
1	0.3818	0.0752	0.4211	3.475	3.498	302.9	40.594
2	0.3812	0.0756	0.4217	3.441	3.435	301.0	40.672
3	0.3816	0.0750	0.4219	3.472	3.560	308.1	40.541
4	0.3814	0.0751	0.4216	3.461	3.468	302.6	40.736
5	0.3817	0.0753	0.4210	3.482	3.524	303.8	40.496
6	0.3820	0.0749	0.4218	3.533	3.551	305.1	40.950
Average: $\Delta_d H_1$ = (40.665 ± 0.067) kJ mol^{-1}							

[a] W / g is mass of sample. ΔE_e/mV, the voltage change during the electrical calibration. ΔE_s/mV, the voltage change during the sample dissolution. $\Delta_s E_m = (\Delta E_s/\Delta E_e) \cdot I^2 R t_e (M/W)$, where R is the electric resistance of the heater (R = 1350.3 Ω at T = 298.15); I, the electrical current (I = 9.997 mA); M, the molar mass; t, heating period of electrical calibration.

Table 6. Dissolution enthalpy of the mixture {$[Er_2(Gly)_2(H_2O)_{12}](ClO_4)_6$ $4H_2O$(s) + 6NaCl(s)} at T = 298.15 K

No	$W_{target\ complex}$ (g)	W_{NaCl} (g)	ΔE_s (mV)	ΔE_s (mV)	t (s)	$\Delta_d H_2$ (kJ mol^{-1})
1	0.6850	0.1751	3.079	3.061	160.7	43.629
2	0.6847	0.1756	3.088	3.063	160.1	43.558
3	0.6843	0.1753	3.094	3.087	161.8	43.752
4	0.6846	0.1750	3.101	3.025	158.2	43.748
5	0.6851	0.1752	3.148	3.064	158.0	43.787
6	0.6848	0.1753	3.097	3.020	157.8	43.660

$\Delta_r H_m = [2\Delta_{sol}H_2 - (\Delta_{sol}H_2 + 2\Delta_{sol}H_3)] =$ (37.641 0.139) kJ mol^{-1}.

A reaction scheme used to derive the standard molar enthalpy of formation of the complex $[Er_2(L\text{-}Gly)_2(H_2O)_{12}](ClO_4)_6 \cdot 4H_2O$(s) has given in Table 7. The enthalpy change of the reaction (3) obtained from experimental values of all the dissolution enthalpies were combined with some auxiliary thermodynamic data, $\Delta_f H_m^o$ [H_2O, l] = – (285.83 0.04) kJ mol^{-1},[12] $\Delta_f H_m^o$ [NaCl, s] = – 411.12 kJ mol^{-1},[12] $\Delta_f H_m^o$ [$NaClO_4 \cdot H_2O$, s] = –677.766 kJ mol^{-1}, [13] $\Delta_f H_m^o$ [$ErCl_3 \cdot 6H_2O$, s] = –2874.41 kJ mol^{-1} and $\Delta_f H_m^o$ [L-Gly, s] = – (527.5 ± 0.5) kJ mol^{-1}, [13£¬14] to drive the standard molar enthalpy of formation of the complex $[Er_2(Gly)_2(H_2O)_{12}](ClO_4)_6 \cdot 4H_2O$(s), $\Delta_f H_m^o$ {$[Er_2(Gly)_2(H_2O)_{12}](ClO_4)_6 \cdot 4H_2O$, s} = ΔH_9 = [$2\Delta H_1$ – (ΔH_2 + $2\Delta H_3$)] + ($2\Delta H_4$ + $2\Delta H_5$ + $6\Delta H_6$ – $2\Delta H_7$ – $6\Delta H_8$) = $\Delta_r H_{m,1}$ + $2\Delta_f H_m^o$ [$ErCl_3 \cdot 6H_2O$, s] + $2\Delta_f H_m^o$ [L-Gly, s] + $6\Delta_f H_m^o$ [$NaClO_4 \cdot H_2O$, s] – $2\Delta_f H_m^o$ [H_2O, l] – $6\Delta_f H_m^o$ [NaCl, s] = –(7794.40 1.01) kJ mol^{-1}, where ΔH_1 – ΔH_9 were the enthalpy changes of the corresponding reactions in the Table 7.

The results of UV-Vis Spectra and Refrangibility (Refractive index) were two important information for detecting the differences of the structure and composition between two kinds of solutions. In this paper, all of the reactants and products of the reaction (3) can be easily dissolved in the selected solvent. The measured values of the refractive indexes of Solution A and Solution A' were (1.5867 ± 0.0012) and (1.5871 ± 0.0009), respectively. The results of UV-Vis Spectroscopy were shown in Figure

Table 7. Reaction Scheme used to determine the standard molar enthalpy of formation of the complex $[Er_2(Gly)_2(H_2O)_{12}](ClO_4)_6 \cdot 4H_2O$(s) at T = 298.15 K

No	Reaction scheme	$\Delta_f H_m^o$ or $\Delta_d H \pm \sigma_a$(kJ mol^{-1})
1	{$2ErCl_3$ $6H_2O$(s)+2Glu(s)+6$NaClO_4$ H_2O(s)} + "s" = Solution A	(40.665 ± 0.067), (ΔH_1)
2	{$[Er_2(Gly)_2(H_2O)_{12}](ClO_4)_6$ $4H_2O$(s)+6NaCl(s)} +"s" = Solution A'	(43.689 ± 0.036), (ΔH_2)
3	Solution A" + {7H2O(l)} = Solution A	0, (ΔH_3)
4	Er(s) + 3/2C_{12}(g) + 3O_2(g) + 6H_2(g) = $ErCl_3$ $6H_2O$(s)	– 2874.41, (ΔH_4)
5	2C(s) + 1/2N_2(g) + 2O_2(g) + 5/2H_2(g) = L-Gly(s)	– (527.5 ± 0.5), (ΔH_5)
6	Na(s) + 1/2Cl_2 + 5/2O_2 + H_2 = $NaClO_4$ H_2O(s)	– 677.766, (ΔH_6)
7	1/2O_2(g) + H_2(g) = H_2O (l)	– (285.83 ± 0.04), (ΔH_7)
8	Na(s) + 1/2Cl_2(g) = NaCl(s)	– 411.12 kJ mol^{-1}, (ΔH_8)
9	2Er(s)+4C(s) + N_2(g) + 22O_2(g) + 21H_2(g) + 3Cl_2(g) = $[Er_2(Gly)_2(H_2O)_{12}](ClO_4)_6$ $4H_2O$(s)	– (7794.40 ± 1.01), (ΔH_9)

4. UV/Vis Spectrum and the data of the refractive indexes of Solution A obtained agreed with those of Solution A', no difference in the structure and chemical composition existed between the two solutions. These results have demonstrated that the physical-chemical properties of the solutions A were the same as those of the solution A', the designed Hess thermochemical cycle was reasonable and reliable, and can be used to derive the standard molar enthalpy of formation of the coordination compound $[Er_2(Gly)_2(H_2O)_{12}](ClO_4)_6 \cdot 4H_2O(s)$.

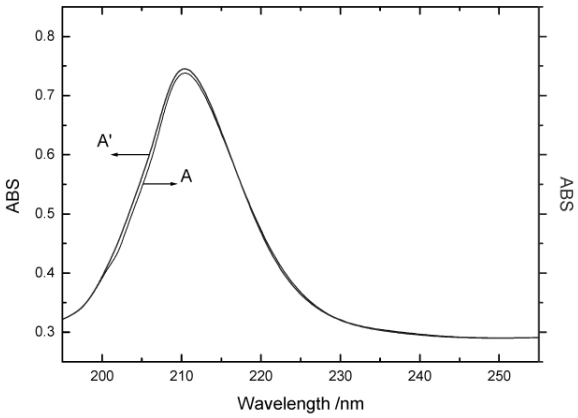

Figure 4. UV-Vis Spectrum of Solution A and Solution A' obtained from the dissolution of the reactants and products in the reaction (1) in 1 mol dm^{-3} HCl (diluted to 1 : 20)

4. Acknowledgements

This work was financially supported by the National Science Foundation of China under the contract NSFC No. 20673050.

5. References

1. B. S. Guo, *Rare Earth*, **1999**, *20*, 64–68.
2. Z. M Wang, *Rare Earth*, **1992**, *13*, 39–43.
3. H. G. Brittain, *Inorg. Chem.*, 1979, *18*, 1740–1745.
4. R. Y. Wang, F. Gao and T. Z. Jin, *Chem.*, **1996**, *10*, 14–18.
5. W. C. Yang, R. Y. Wang, T. Z. Jin, Z. Y. Zhou and X. G. Zhou, *J. Rare Earths*, **1998**, *16,* 11–16.
6. Z. C. Tan, G. Y. Sun, A. X. Yin, W. B. Wang, J. C. Ye and L. X. Zhou, *J. Therm. Anal.*, **1995**, *45*, 59–67.
7. G. A. Donald, *J. Phys. Chem. Ref. Data*, **1993**, *22,* 1441–1453.
8, Y. Y. Di, Z. C. Tan, S. L.Gao and S. X. Wang, *J. Chem. Eng. Data*, **2004**, *49*, 965–969.
9. Y. Y. Di, S. L. Gao, L. W. Li, Z. C. Tan and S. L. Gao, *J. Chem. Thermodyn.*, **2006**, *38*, 884–888.
10. R. Rychly and V. Pekarek, *J. Chem. Thermodyn.*, **1977**, *9*, 391–396.
11. J. Xing, Z. C. Tan, Y. Y. Di, X. H. Sun, L. X. Sun and T. Zhang, *Acta Chim. Sinica.*, **2004**, *62*, 2414–2419.
12. R. C. Weast: Handbook of Chemistry and Physics, CRC Press, Florida, **1989**, D–121.
13. J. A. Dean: Lange's Handbook of Chemistry, 12th Edn., Mc Graw-Hill Book Co., New York, **1979**, 9–2.
14. V. P. Vasilev, V. A. Borodin and S. B. Kopnyshev, *Russ. J. Phys. Chem. (Engl. Transl.)*, **1991,** *65*, 29–32.

Povzetek

Pripravili smo kompleks erbijevega perklorata z L–glicinom, $[Er_2(Gly)_2(H_2O)_{12}] (ClO_4)_6 4H_2O$. Kompleksu smo z avtomatskim adiabatnim kalorimetrom določili nizkotemperaturno toplotno kapaciteto v temperaturnem območju 78 do 372 K. V temperaturnem območju 275 ~ 296 K smo opazili proces, ki smo ga pripisali faznemu prehodu kompleksa v trdnem stanju s temperaturo 283,315 ± 0,061 K, spremembo entalpije 11,026 0,059 kJ mol^{-1} in spremembo entropije 38,918 ± 0,206 J K^{-1} mol^{-1}. Toplotne kapacitete v območju 78 ~ 275 K in 296 ~ 372 K se lahko izrazijo kot polinoma. Standardna tvorbena entalpija kompleksa, določena s kalorimetrijo in upoštevanjem Hessovega zakona znaša $\Delta_f H_m^o$ – (7794.40 ± 1.01) kJ mol^{-1}.